

Spectroscopic rotational velocities of brown dwarfs

M. R. Zapatero Osorio¹

LAEFF-INTA, P. O. 50727, E-28080 Madrid, Spain

mosorio@laeff.inta.es

E. L. Martín² and H. Bouy

IAC, Vía Láctea s/n, E-38205 La Laguna, Tenerife, Spain

ege@iac.es, bouy@iac.es

R. Tata, R. Deshpande

University of Central Florida, Dept. of Physics, P. O. 162385, Orlando FL 32816-2385, USA

tata@physics.ucf.edu, rohit@physics.ucf.edu

and

R. J. Wainscoat

Institute for Astronomy, 2680 Woodlawn Drive, Honolulu, HI 96822, USA

rjw@ifa.hawaii.edu

ABSTRACT

We have obtained projected rotation velocities ($v_{\text{rot}} \sin i$) of a sample of 19 ultracool dwarfs with spectral types in the interval M6.5–T8 using high-resolution, near-infrared spectra obtained with NIRSPEC and the Keck II telescope. Among our targets there are two young brown dwarfs, two likely field stars, and fifteen likely brown dwarfs ($30\text{--}72M_{\text{Jup}}$) of the solar neighborhood. Our results indicate that the T-type dwarfs are fast rotators in marked contrast to M-type stars. We have derived $v_{\text{rot}} \sin i$ velocities between ≤ 15 and 40 km s^{-1} for them, and have found no clear evidence for T dwarfs rotating strongly faster than L dwarfs. However, there is a hint for an increasing lower envelope on moving from mid-M to the L spectral types in the $v_{\text{rot}} \sin i$ –spectral type diagram that was previously reported in the literature; our $v_{\text{rot}} \sin i$ results extend it to even cooler types. Assuming that field brown dwarfs have a size of $0.08\text{--}0.1 R_{\odot}$, we can place an upper limit of 12.5 h on the equatorial rotation period of T-type brown dwarfs. In addition, we have compared our $v_{\text{rot}} \sin i$ measurements to spectroscopic rotational velocities of very young brown dwarfs of similar mass available in the literature. The comparison, although model-dependent, suggests that brown dwarfs lose some angular momentum during their contraction; however, their spin down time seems to be significantly longer than that of solar-type to early-M stars.

Subject headings: stars: low-mass, brown dwarfs — stars: rotation — individual (PPl 1, 2MASS J03341218-4953322, vB 10, LP 944-20, 2MASS J00361617+1821104, 2MASS J22244381-0158521, SDSS J053951.99-005902.0, 2MASS J17281150+3948593AB, 2MASS J16322911+1904407, DENIS-P J0255.0-4700, SDSSp J125453.90-012247.4, 2MASS J05591914-1404488, 2MASS J15031961+2525196, SDSS J134646.45-003150.4, SDSS J162414.37+002915.6, 2MASS J15530228+1532369AB, 2MASS J12171110-0311131, GL 570D, 2MASS J04151954-0935066)

1. Introduction

Rotation is a key parameter fundamental in examining stellar activity and angular momentum evolution. The rotation of stars has been studied for nearly all spectral types and for a wide range of ages. These studies have contributed to our knowledge of the stellar angular momentum history. In particular, field early-M dwarfs are amongst the slowest rotating stars on the main sequence with typical projected rotational velocities ($v_{\text{rot}} \sin i$) below 5 km s^{-1} (e.g., Marcy & Chen (1992); Delfosse et al. (1998)). It has been suggested that many of these stars lose about 98% of their angular momentum during their lifetimes via magnetic activity, winds and mass loss. However, very little is known about the rotation rate and angular momentum evolution of brown dwarfs.

The state-of-the-art evolutionary models by Baraffe et al. (2003) and Burrows et al. (1997) predict that a star at the substellar mass limit ($0.072 M_{\odot}$, or $\sim 72 M_{\text{Jup}}$) reaches the hydrostatic equilibrium at an effective temperature of about 1800 K. However, T-type dwarfs (for the spectral definition see Burgasser et al. (2002a) and Geballe et al. (2002)) are characterized by surface temperatures cooler than $\sim 1300 \text{ K}$ (Vrba et al. (2004); Nakajima, Tsuji, & Yanagisawa (2004)). Hence, T-type dwarfs are all believed to be brown dwarfs because they have cooled down even below the minimum atmospheric temperature of the smallest stars. On the basis of theoretical predictions and very recent temperature calibrations (e.g., Dahn et al. (2002)), the star–brown dwarf frontier happens at spectral type L3–L4 at ages of a few Gyr. Field objects with later types are probably substellar. Various efforts have been made so far to derive the rotational velocity of L-type dwarfs (e.g., Basri et al. (2000); Reid et al. (2002); Mohanty et al. (2003); Bailer-Jones (2004)). In contrast to early- and mid-M stars, L dwarfs appear to be relatively fast rotators with $v_{\text{rot}} \sin i$ values in the range $10\text{--}60 \text{ km s}^{-1}$. To the best of our knowledge, only the binary T1/T6 ϵ Indi Bab has a rotation velocity measurement available in the literature: $v_{\text{rot}} \sin i = 28 \text{ km s}^{-1}$ (determined for

the unresolved system, Smith et al. (2003)).

This paper presents high-resolution, near-infrared spectroscopic observations of 19 bright, ultracool dwarfs with spectral types in the interval M6.5–T8. Our analysis is intended to first, determine the rotational velocity of brown dwarfs, with particular emphasis on the late-L and T-type dwarfs, and second, study the change of rotation rate from very young ages to the ages typical of the solar neighborhood, which will allow us to obtain new insight on the angular momentum evolution in the substellar regime.

2. The sample, observations and data reduction

The sample of targets is listed in Table 1. It comprises 4 late-M type dwarfs, two of which are young and lithium-bearing brown dwarfs (PP11 is a member of the Pleiades cluster, Stauffer, Schultz, & Kirkpatrick (1998); and LP 944–20 is a likely member of the Castor moving group, Tinney (1998); Ribas (2003)). The remaining targets are 6 L- and 9 T-type field dwarfs recently discovered by the 2MASS, SLOAN and Denis surveys; discovery papers are provided in the last column of Table 1. The spectral types given in the second column of Table are taken from the literature (Kirkpatrick, Henry, & Simons (1995); Kirkpatrick, Henry, & Irwin (1997); Kirkpatrick et al. (1999), (2000); Martín et al. (1999); Geballe et al. (2002); Burgasser et al. (2006); Phan-Bao et al. (2006)). They were derived from optical and/or near-infrared low-resolution spectra and are in the interval M6.5–T8. There are objects that have been typed differently by the various groups; we provide all classifications in Table 2, first the one from Kirkpatrick et al. (1999) or Burgasser et al. (2006), second the one from Geballe et al. (2002), and finally, the classification from Martín et al. (1999). For those targets with the largest discrepancies (J1632+19 and J0255–47), we will adopt their mean spectral type to produce the figures of this paper. In terms of effective temperature, our sample spans the range 2700–770 K (Leggett et al. (2000a); Vrba et al. (2004)). J0334–49 and vB 10 can be stars in our sample while the remaining targets are very likely substellar.

We collected high-resolution near-infrared spectra of the 19 ultracool dwarfs using the Keck

¹Also at IAC, Vía Láctea s/n, E-38205 La Laguna, Tenerife, Spain

²Also at University of Central Florida, Dept. of Physics, P. O. 162385, Orlando FL 32816-2385, USA

II telescope and the NIRSPEC instrument, a cross-dispersed, cryogenic echelle spectrometer employing a 1024×1024 ALADDIN InSb array detector. These observations were carried out on different occasions from 2000 December through 2006 January and are part of our large program aimed at the study of radial velocity variability. The log of the observations is shown in Table 1. In the echelle mode, we selected the NIRSPEC-3 (*J*-band) filter, and an entrance slit width of $0''.432$ (i.e., 3 pixels along the dispersion direction of the detector), except for eight targets (J2224–01, J1728+39, J1632+19, J1346–00, J1624+00, J1553+15, J1217–03, and GL 570D) for which we used an entrance slit width of $0''.576$. The length of both slits was $12''$. All observations were performed at an echelle angle of $\sim 63^\circ$. This instrumental setup provided a wavelength coverage from 1.148 up to $1.346 \mu\text{m}$ splitted into ten different orders, a nominal dispersion ranging from 0.164 (blue wavelengths) to $0.191 \text{ \AA}/\text{pix}$ (red wavelengths), and a final resolution element of $0.55\text{--}0.70 \text{ \AA}$ at $1.2485 \mu\text{m}$ (roughly the central wavelength of the spectra), corresponding to a resolving power $R \sim 17800\text{--}22700$. Individual exposure times were function of the brightness of the targets, ranging from 120 to 900 s.

Raw data were reduced using the ECHELLE package within IRAF¹. Spectra were collected at two or three different positions along the entrance slit. Nodded images were subtracted to remove sky background and dark current. White-light spectra obtained with the same instrumental configuration and for each target were used for flat-fielding the data. All spectra were calibrated in wavelength using the internal arc lamp lines of Ar, Kr, and Xe, which were typically acquired after observing the targets. The vacuum wavelengths of the arc lines were identified and we produced fits using a third order Legendre polynomial along the dispersion axis and a second order one perpendicular to it. The mean rms of the fits was 0.03 \AA , or 0.7 km s^{-1} . We note that any systematic error or different zero point shifts that may be present in the instrumental calibration does not affect the rotational velocity measurements. In or-

der to correct for atmospheric telluric absorptions, near-infrared featureless stars of spectral types A0–A2 were observed several times and at different air masses during the various observing runs. The hydrogen line at $1.282 \mu\text{m}$, which is intrinsic to these hot stars, was removed from the spectra before using them for division into the corresponding science data. Finally, we multiplied the science spectra by the black body spectrum for the temperature of 9480 K, which is adequate for A0V type (Allen (2000)). We plotted in Fig. 1 example spectra of our targets around the KI doublet at $1.2485 \mu\text{m}$. Effective temperature (i.e., spectral type) decreases from top to bottom. Note that all spectra have been shifted in velocity to vacuum wavelengths for a facile comparison of the atomic and molecular features. The signal-to-noise ratio of the spectra varies for different echelle orders and different targets depending on their brightness. In general, the red orders show better signal-to-noise ratio than the blue orders, except for the reddest order centered at $1.337 \mu\text{m}$ in T dwarfs, since these wavelengths are affected by strong methane and water vapor absorptions below 1300 K.

3. Rotational velocities

We measured projected rotational velocities via a cross-correlation of the spectra of our targets against spectra of slowly rotating dwarfs of similar types. The details of the procedure, which is based on the assumption that the line broadening is dominated by rotation, is fully described in the literature (e.g., Reid et al. (2002); Bailer-Jones (2004), and references therein). Summarizing, rotational velocities, $v_{\text{rot}} \sin i$, are obtained from the width of the peak of the cross-correlation function between the targets and the slow rotator templates. The larger the width, the faster the rotation rate. We performed the cross-correlation on each order separately, fit a Gaussian to the peak, and measured its width, which is calibrated against $v_{\text{rot}} \sin i$ by applying artificial broadening for a range of velocities (10 up to 50 km s^{-1} in steps of 5 km s^{-1}) to the spectra of slow rotators. We adopted the line rotation profile given by Gray (1992), and a limb darkening parameter of $\epsilon = 0.6$. One example of the artificially broadened spectra is displayed in Fig. 2 (bottom spectrum). Only orders for which we unambiguously identified the peak of the cross-correlation function and ob-

¹IRAF is distributed by National Optical Astronomy Observatory, which is operated by the Association of Universities for Research in Astronomy, Inc., under contract with the National Science Foundation.

tained good fits were used. Then, all results were averaged to produce the final $v_{\text{rot}} \sin i$ measurement. Uncertainties are derived from the standard deviation of the mean.

Ideally, non-rotating templates should be used. Mohanty & Basri (2003) reported a very low projected velocity of the M8V-type star vB 10 ($v_{\text{rot}} \sin i = 6.5 \text{ km s}^{-1}$). This is well below the instrumental profile broadening of our data, which is about 15 km s^{-1} based on one pixel resolution, and is also smaller than the minimum detectable rotation from our data (see below). As a result, vB 10 can be considered a non-rotator in our study, and has been employed as a template to obtain rotational velocities of the M- and L-type targets. The cross-correlation technique assumes that the target and template spectra are of similar type and differ only in the rotation velocity. Nevertheless, Bailer-Jones (2004) has recently shown that M-type templates can also yield accurate rotation velocities of L dwarfs. In our sample, the energy distribution of T dwarfs do differ significantly from M dwarfs, and we found that for the T-type targets the cross-correlation with vB 10 gives reasonable results if resonance lines of K I are avoided and only molecular (particularly water vapor) lines are used in the cross-correlation. The cool brown dwarf J1346–00 (T6.5V) turns out to have a low value of $v_{\text{rot}} \sin i$ (because of the unknown inclination angle of the rotation axis, we cannot establish whether J1346–00 is a true fast or slow rotator. However, we used it as a “slow rotator” in our study). From the data we can impose an upper limit of 15 km s^{-1} on its projected rotational velocity. We used J1346–00 as a secondary template to measure rotational broadening of the coolest objects in our sample, the late-L and T-type dwarfs. We note, however, that using a rotating template will underestimate the rotation velocities (Mohanty & Basri (2003) provide an extensive and quantitative discussion on this respect). Our derived $v_{\text{rot}} \sin i$ measurements using vB 10 and J1346–00 as the slowly rotating reference objects are given in columns 3 and 4 of Table 2, respectively. The agreement between the two columns is good within $1\text{-}\sigma$ the uncertainty (i.e., there is no obvious tendency for $v_{\text{rot}} \sin i$ obtained using J1346–00 to be lower than the values derived with the M-type dwarf). For those objects in common with other studies (2 M dwarfs and 4

L dwarfs), we also give their previously derived projected rotational velocities in column 5 of Table 2. With the only exception of J0036+18 (see below), our measurements and the values from the literature agree within the expected errors.

Figure 2 depicts the spectra of the T-type secondary template (J1346–00) and of one rapid rotator of similar classification (J1624+00, T6V). The data of J1624+00 were shifted in velocity to match the template. For comparison purposes, the spectrum of J1346–00 broadened at the (roughly) rotation velocity of J1624+00 is also shown at the bottom of the Figure. The resemblance of J1624+00 to the artificially broadened spectrum is remarkable, supporting the $v_{\text{rot}} \sin i$ results of the cross-correlation technique.

In our sample of 19 ultracool dwarfs, only 3 of them have small values of $v_{\text{rot}} \sin i$: the reference M8-type dwarf vB 10, the nearby M9-dwarf J0334–49, and the T6.5-type object J1346–00. For the latter two we have placed an upper limit of 15 km s^{-1} . The cross-correlation technique suggests that the M9-dwarf rotates at a speed of $8.5 \pm 2.6 \text{ km s}^{-1}$. However, this measurement is below the minimum detectable projected rotational velocity of our study, which we estimate at about 10.5 km s^{-1} after the discussion by Bailer-Jones (2004). Therefore, the adoption of the mean NIRSPEC instrumental broadening as the upper limit on the $v_{\text{rot}} \sin i$ for the slowest rotators in our sample is conservative. It may be noteworthy that we have found a slowly rotating T dwarf in a sample of 9 T-type dwarfs, while a much larger sample of L dwarfs drawn from our work and the literature has yet to yield one. However, we note that there are a few L-dwarfs with $v_{\text{rot}} \sin i \sim 10 \text{ km s}^{-1}$, and that the rotation inclinations are randomly distributed.

4. Discussion

4.1. Periodic photometric variability and $v_{\text{rot}} \sin i$

Four L-type dwarfs among our targets have tentative rotational periods available in the literature. Berger et al. (2005) reported on the detection of strongly variable and periodic radio emission in J0036+18 (L3.5V) with a periodicity of 3 h. These authors suggested various scenarios to account for the observed periodic radio emission, one of which

is related to equatorial rotation and an anchored, long-lived magnetic field. The period of 3 h is consistent with our $v_{\text{rot}} \sin i$ measurement ($36.0 \pm 2.7 \text{ km s}^{-1}$); thus, it is plausibly the true rotation periodicity. Using a radius of $0.09 R_{\odot}$, the inferred inclination angle of the rotation axis is $i \geq 66^{\circ}$ with an expectation value of 81° . We note, however, that our $v_{\text{rot}} \sin i$ differs by a factor of 2.4 with respect to the measurement given by Schweitzer et al. (2001). These authors employed a different technique to determine rotation velocities: they compared artificially broadened theoretical spectra to observed spectra. Using a similar approach, Jones et al. (2005) obtained a rotation velocity (see Table 2) in better agreement with our measurement.

Recently, Koen (2005) has discussed the possible variable nature of J0255–47 (L9V/dL6) on more than one timescale. This author found two possible photometric modulations with periodicities of 1.7 and 5.2 h in the optical light curve of J0255–47. If this object has a radius of $0.09 R_{\odot}$, the longest period may be ruled out as the rotation period. However, the shortest periodicity is consistent with a rotational modulation, and when combined with our $v_{\text{rot}} \sin i$ would yield a rotation axis inclination angle of $i \sim 40^{\circ}$. Then, the true equatorial velocity of J0255–47 would turn out to be $\sim 64 \text{ km s}^{-1}$.

The L5V dwarf J0539–00 has also been detected to be photometrically variable by Bailer-Jones & Mundt (2001), with a derived periodicity of 13.3 h. And a tentative modulation of 21.8 h associated to the L4.5V dwarf J2224–01 has been reported by Gelino et al. (2002). Given our $v_{\text{rot}} \sin i$ data and the radius of $0.09 R_{\odot}$, such long periods cannot be securely ascribed to rotation modulation of a long-lived atmospheric feature. Similarly, other ultracool dwarfs show too long periodic variability to be related to the rotation period (e.g., Martín, Zapatero Osorio, & Lehto (2001); Gelino et al. (2002)). Nevertheless, long periodicities could be interpreted as due to equatorial rotation if these objects had larger size, i.e., were significantly younger than the rest of the objects in the solar neighborhood.

4.2. Rotation and angular momentum evolution

From Table 2, field T-type brown dwarfs are relatively fast rotators with $v_{\text{rot}} \sin i$ measurements

in the interval $\leq 15\text{--}40 \text{ km s}^{-1}$. All state-of-the-art evolutionary models available in the literature predict that the size of brown dwarfs keeps approximately constant ($0.08\text{--}0.1 R_{\odot}$) at ages older than $\sim 0.5 \text{ Gyr}$ regardless the mass. Under the assumption that this theoretical prediction is correct, the rotation periods of T-type brown dwarfs are probably below 12.5 h. To date, only a few T dwarfs have been photometrically monitored to search for rotational modulation (e.g., Burgasser et al. (2002a); Goldman (2003); Koen (2005)). Enoch, Brown, & Burgasser (2003) found evidence for periodic behavior on a timescale of 3 h in one T1 brown dwarf. Unfortunately, this variable object is not in our sample; nevertheless, the derived photometric periodicity is consistent with our prediction for T-type brown dwarfs based on the radii given by the evolutionary models.

Our $v_{\text{rot}} \sin i$ results are plotted against spectral type in Fig. 3, where we have also included data of field M stars and L dwarfs from the literature (Marcy & Chen (1992); Basri & Marcy (1995); Delfosse et al. (1998); Basri et al. (2000); Reid et al. (2002); Mohanty & Basri (2003); Bailer-Jones (2004)). The $v_{\text{rot}} \sin i$ measurement of the unresolved T-dwarf binary ϵ Indi Bab obtained by Smith et al. (2003) is also plotted in the Figure. Note that many early-M to mid-M stars have very slow rotation ($v_{\text{rot}} \sin i \leq 5 \text{ km s}^{-1}$, Delfosse et al. (1998); Mohanty & Basri (2003)), and for the sake of clarity we have not plotted in the Figure the upper limits on their detection. It is obvious that there is a correlation between rotation and spectral type: rotational velocity keeps increasing with later spectral type from M to T types. This behavior was previously reported for M and L dwarfs in the literature (Mohanty & Basri (2003); Bailer-Jones (2004)), and is in part due to the different mass of the objects contemplated in Fig. 3. We will not consider the young brown dwarfs of our sample, PP11 and LP 944–20, in the following discussion. At the typical age interval of the solar vicinity ($\sim 1\text{--}10 \text{ Gyr}$), T-type objects are substellar with likely masses in the brown dwarf regime ($20\text{--}70 M_{\text{Jup}}$, Baraffe et al. (2003)). On the contrary, and for the same age interval, low-mass and very low-mass field stars above the substellar limit have M and early-L types. From Fig. 3, and despite the uncertainty introduced by the inclination angle of the rotation axis, field brown dwarfs in-

deed rotate more rapidly than field M-type stars. Scholz & Eislöffel (2004) and (2005) studied the rotation period–mass relationship of stellar and substellar members in the σ Orionis and ϵ Orionis young clusters finding that the lower the mass, the shorter the rotation period.

Field L-type dwarfs can be either very low-mass stars with probable masses below $0.1 M_{\odot}$ or brown dwarfs depending on age and surface temperature. About 35% of L3V–L4V dwarfs have lithium in their spectra, and the rate increases up to 70% at L6V (Kirkpatrick et al. (2000)). These are definitively substellar with likely masses below $60 M_{\text{Jup}}$. L-type objects are also reported in the literature to be fast rotators (Basri et al. (2000); Bailer-Jones (2004)), with projected rotational velocities up to 60 km s^{-1} , and a minimum velocity of 10 km s^{-1} (Mohanty & Basri (2003)). From our data, T-type brown dwarfs do not appear to have significantly faster rotation than L dwarfs, and a smooth transition between the L- and T-types can be seen in Fig. 3. However, we note that there is a hint for the lower envelope of the $v_{\text{rot}} \sin i$ –spectral type relation to increase linearly from mid-M to T types. This trend may be an artifact of the small sample size of T dwarfs and of our detection limit; hence, more measurements of different T-type brown dwarfs would be required to definitively ascertain this tendency.

Also relevant is the exploration of the angular momentum evolution of brown dwarfs. To address this issue we should know the age of our sample. PP11 is a Pleiades brown dwarf ($60\text{--}72 M_{\text{Jup}}$) with an estimated age of 120 Myr. We have calculated the space motions of all the other targets except for two T dwarfs that lack parallax measurements (forthcoming paper), and used the criteria defined by Leggett (1992) to group them into young disk, young-old disk and old disk kinematic categories. LP 944–20 was widely discussed by Ribas (2003). According to their galactic velocities, all L and T dwarfs of Table 2 can be classified as members of the young and young-old disk, for which we have assumed the following age intervals: 0.6–1.5 Gyr (young disk) and 1–5 Gyr (young-old disk). We note that Reid et al. (2002) also pointed out that late-M dwarfs appear kinematically younger than early-M stars, and that young M dwarfs rotate faster than the older ones. From our data, we find no difference in $v_{\text{rot}} \sin i$ between the young disk

T dwarfs and the young-old disk ones.

Our $v_{\text{rot}} \sin i$ values are plotted against age in Fig. 4, where we have considered only brown dwarfs (PP11, LP 944–20, and the field dwarfs cooler than L3.5V). Further spectroscopic rotation velocities of confirmed lithium-bearing Pleiades brown dwarfs and of the substellar pair GJ 569Ba and GJ 569Bb are obtained from the literature (Basri & Marcy (1995); Martín et al. (1998); Zapatero Osorio et al. (2004)), and are also shown in the Figure. Despite the scarce number of data for ages of hundred Myr, there is no clear evidence for a significant braking between the Pleiades age and the field. This contrasts markedly to solar-type stars. At the age of the Hyades (~ 600 Myr), most G- and K-type stars are rather slow rotators, and some M-type stars display relatively rapid rotation with maximum $v_{\text{rot}} \sin i = 20 \text{ km s}^{-1}$ (Stauffer et al. (1997)).

We have compiled the $v_{\text{rot}} \sin i$ measurements of very young brown dwarfs with ages between ~ 1 and 10 Myr from Joergens & Guenther (2001), Muzerolle et al. (2003), and Mohanty, Jayawardhana & Basri (2005). These data correspond to confirmed substellar members of the following star-forming regions and young clusters: ρ Ophiuchi (~ 1 Myr), Taurus (~ 1.5 Myr), IC 348 (~ 2 Myr), Chamaeleon I (~ 2 Myr), σ Orionis (~ 3 Myr), Upper Scorpius (~ 5 Myr), and TW Hya (~ 10 Myr). It is accepted that the substellar limit is located at about M6–M6.5 spectral type at these young ages as well as in the Pleiades (e.g., Luhman et al. (1998); Martín et al. (1998)). Hence, to secure that only brown dwarfs are depicted in Fig. 4, we have plotted sources with spectral type M7 and later (the coolest brown dwarf of these spectroscopic studies has spectral class M9.5). Their masses are likely in the interval $30\text{--}70 M_{\text{Jup}}$, i.e., fully overlapping with the mass estimates for the field T-type objects of our sample. The projected rotation velocities of the very young (≤ 10 Myr) brown dwarfs span the range $0\text{--}60 \text{ km s}^{-1}$. In addition, several groups have photometrically monitored substellar members of the σ Orionis and ϵ Orionis (~ 6 Myr) clusters (Bailer-Jones & Mundt (2001); Scholz & Eislöffel (2004), (2005); Zapatero Osorio et al. (2003); Caballero et al. (2004)), finding periodic behaviors on timescales between 3 and 80 h. The various groups of authors discuss that

the observed modulated variability is possibly related to rotation in many cases. We have used the radii predictions of Baraffe et al. (2003) to transform periods into velocities, which are plotted as arrows (denoting upper limits) in Fig. 4. From the Figure, it is noteworthy that a significant amount ($\sim 50\%$) of young, massive brown dwarfs have $v_{\text{rot}} \sin i \leq 10 \text{ km s}^{-1}$, while, in general, field substellar objects of similar mass rotate three to six times faster. Brown dwarfs definitively undergo a spin-up because of gravitational contraction, and their spin-down time appears to be longer than that of solar-type stars. Chabrier & Küker (2006) argued that the magnetic field topology of fully convective objects exhibits an asymmetric structure, which in addition to the decreasing conductivity in the atmosphere of ultracool dwarfs reduces the efficiency of magnetic braking, providing a possible explanation for the lower angular momentum loss of brown dwarfs.

Nevertheless, fast-rotating brown dwarfs do exist at all ages from a few Myr through several Gyr. This is independent of evolutionary models, since rotation periods of a few hours and $v_{\text{rot}} \sin i \geq 10 \text{ km s}^{-1}$ are equally observed among young and field brown dwarfs. This suggests some angular momentum loss throughout the lifetime of a brown dwarf. Furthermore, with the current evolutionary models, simple hydrostatic contraction (i.e., angular momentum conservation) fails to reconcile the entire $v_{\text{rot}} \sin i$ distributions of the young ($\leq 10 \text{ Myr}$) and “old” ($\geq 100 \text{ Myr}$) substellar populations shown in Fig. 4. As an example, we have plotted in the $v_{\text{rot}} \sin i$ -age diagram of Fig. 4 the purely hydrostatic contraction of two presumed brown dwarfs with masses of 30 (dashed line) and 60 M_{Jup} (solid line) by assuming a moderate “initial” rotation velocity of 9 km s^{-1} and the theoretical models of Baraffe et al. (2003). We note that 60 M_{Jup} is probably the most representative mass of the objects in Fig. 4. At the very young ages, there are brown dwarfs located above and below the curves of angular momentum conservation; however, for ages older than 1 Gyr, nearly all brown dwarfs lie below the curves. Hence, some braking becomes apparent. We remark that the conclusions drawn from this discussion are based on current evolutionary models, and should be revised if the models are proved to be wrong.

The fastest rotating young brown dwarfs with masses in the interval 50–72 M_{Jup} , periods below 10 h, and $v_{\text{rot}} \geq 45 \text{ km s}^{-1}$ (note the drop of $\sin i$) pose a problem to theory (Scholz et al. (2005)). Relying on actual models, these rapid, massive substellar rotators would reach the spherical breakup velocity in less than the lifetime of the Galaxy unless they brake down dramatically. It is expected that fast rotation impacts the evolution of brown dwarfs. These objects have rather neutral atmospheres (low conductivity) and despite the fact they can hold some long-lived magnetic fields up to a few Gyr (Berger et al. (2005), and references therein), the atmospheric fluid motions and the field are likely decoupled, which reduces the “magnetic” activity. The mechanisms through which ultracool (particularly the L and T types), fully convective rotators can lose angular momentum are to be determined (magnetic braking, frictional heating, etc.). However, it is worth mentioning that young massive brown dwarfs of mid- to late-M spectral classes are warm enough to have coronae in a similar manner than low-mass stars (see, e.g., Preibisch & Zinnecker (2002); Mokler & Stelzer (2002); Bouy (2004); Preibisch et al. (2005), and references therein). This could in principle provide a braking mechanism but at a time when the brown dwarfs have not yet fully contracted and have not cooled down significantly. Because there is no obvious braking between the Pleiades and field brown dwarfs (Fig. 4), it might be possible that these objects spin up due to contraction and brake down while still being warm (and very young), and once they evolve to cooler temperatures the braking time becomes longer. Very recently, Reiners & Basri (2006) report on the high $v_{\text{rot}} \sin i$ of an halo L-dwarf, suggesting that braking is even inexistent (provided the object has an “halo” age). Additionally, flare activity, like the one reported in a few field L dwarfs (e.g., Liebert et al. (2003)) can also shed off angular momentum. Nevertheless, the frequency of strong flares in cool objects is quite low ($\leq 7\%$, Gizis et al. (2000)), so their contribution to the rotation braking is expected to be small. Finally, we point out that there can be a diversity of angular momentum histories in our sample of brown dwarfs; some could be binaries, some may have flares, etc.

5. Summary and conclusions

We obtained high-resolution ($R \sim 17800\text{--}22700$), near-infrared ($1.148\text{--}1.346\ \mu\text{m}$) spectra of a sample of 19 ultracool dwarfs (M6.5–T8) using the NIRSPEC instrument and the 10-m Keck II telescope. Our sample comprises two late-M dwarfs, two young (100–500 Myr) brown dwarfs and fifteen L3.5–T8 likely brown dwarfs of the solar neighborhood. Projected rotation velocities ($v_{\text{rot}} \sin i$) were measured via a cross-correlation of the data against spectra of slow-rotating dwarf templates of similar types, which were observed with the same instrumental configuration. The star vB 10 (M8V) and the brown dwarf J1346–00 (T6.5V) were the templates. We found that, in general, the T-type brown dwarfs are relatively fast rotators, as are also the L dwarfs, with $v_{\text{rot}} \sin i$ spanning the range $\leq 15\text{--}40\ \text{km s}^{-1}$. Assuming a radius of $0.08\text{--}0.1 R_{\odot}$, we placed an upper limit of 12.5 h on the equatorial rotation of T dwarfs. Rotation appears to correlate with spectral type (from M to T class), $v_{\text{rot}} \sin i$ increasing towards later types. However, we found no clear evidence for T dwarfs rotating significantly faster than L dwarfs.

We compared our $v_{\text{rot}} \sin i$ measurements to photometric periods of four L dwarfs reported in the literature, and concluded that the 3-h periodic radio emission of J0036+18 (Berger et al. (2005)) is likely the true rotation period of the object. However, the derived photometric periodicities of J0255–47 (5.2 h, Koen (2005)), J0539–00 (13.3 h, Bailer-Jones & Mundt (2001)), and J2224–01 (21.8 h, Gelino et al. (2002)) seem too long to be considered the rotation periods if we assume a radius of $0.09 R_{\odot}$.

We also compared our data to $v_{\text{rot}} \sin i$ measurements of brown dwarfs of similar mass (30–72 M_{Jup}), which are confirmed members of very young star-forming regions and star clusters (1–10 Myr). A significant fraction of the very young brown dwarfs show $v_{\text{rot}} \sin i \leq 10\ \text{km s}^{-1}$, which contrasts with the high values found in field brown dwarfs. This supports the fact that brown dwarfs spin up with age due to gravitational contraction. From the calculation of the hydrostatic contraction based on radii predictions of state-of-the-art evolutionary models, we conclude that brown dwarfs seem to brake down from 1 Myr to the age of the solar neighborhood, and hence, they

lose some angular momentum. However, massive brown dwarfs do not appear to brake down as dramatically as solar-type to early-M stars, suggesting that their spin-down time is significantly longer.

We thank V. J. S. Béjar for useful discussions. We also thank G. Basri (the referee of this paper) for his comments and suggestions. This research has been supported by a Keck PI Data Analysis grant awarded to E. L. M. by Michelson Science Center, and by the Spanish projects AYA2003-05355 and AYA2005-06453. We thank the Keck observing assistants and the staff in Waimea for their kind support. The data were obtained at the W. M. Keck Observatory, which is operated as a scientific partnership between the California Institute of Technology, the University of California, and NASA. The Observatory was made possible by the generous financial support of the W. M. Keck Foundation. The authors extend special thanks to those of Hawaiian ancestry on whose sacred mountain we are privileged to be guests. This research has made use of the SIMBAD database, operated at CDS, Strasbourg, France.

REFERENCES

- Allen, W. B. 2000, *Allen’s Astrophysical Quantities*. Fourth edition, ed. Arthur N. Cox, New York: Springer Verlag, p. 151
- Bailer-Jones, C. A. L. 2004, *A&A*, 419, 703
- Bailer-Jones, C. A. L., & Mundt, R. 2001, *A&A*, 367, 218
- Baraffe, I., Chabrier, G., Barman, T. S., Allard, F., & Hauschildt, P. 2003, *A&A*, 402, 701
- Basri, G., Mohanty, S., Allard, F., Hauschildt, P. H., Delfosse, X., Martín, E. L., Forveille, T., & Goldman, B. 2000, *ApJ*, 538, 363
- Basri, G., & Marcy, G. W. 1995, *AJ*, 109, 762
- Berger, E., Rutledge, R. E., Reid, I. N., et al. 2005, *ApJ*, 627, 960
- Bouy, H. 2004, *A&A*, 424, 619
- Burgasser, A. J., Kirkpatrick, J. D., Brown, M. E., et al. 1999, *ApJ*, 522, L65

- Burgasser, A. J., Wilson, J. C., Kirkpatrick, J. D., et al. 2000a, *AJ*, 120, 1100
- Burgasser, A. J., Kirkpatrick, J. D., Cutri, R. M., et al. 2000b, *ApJ*, 531, L57
- Burgasser, A. J., Liebert, J., Kirkpatrick, J. D., & Gizis, J. E. 2002a, *AJ*, 123, 2744
- Burgasser, A. J., Kirkpatrick, J. D., Brown, M. E. et al. 2002b, *ApJ*, 564, 421
- Burgasser, A. J., Kirkpatrick, J. D., McElwain, M. W., Cutri, R. M., Burgasser, A. J., & Skrutskie, M. F. 2003, *AJ*, 125, 850
- Burgasser, A. J., Geballe, T. R., Leggett, S. K., Kirkpatrick, J. D., & Golimowski, D. A. *ApJ*, 637, 1067
- Burrows, A., Marley, M., Hubbard, W. B., Lunine, J. I., Guillot, T., Saumon, D., Freedman, R., Sudarsky, D., & Sharp, C. 1997, *ApJ*, 491, 856
- Caballero, J. A., Béjar, V. J. S., Rebolo, R., & Zapatero Osorio, M. R. 2004, *A&A*, 424, 857
- Chabrier, G., & Küker, M. 2006, *A&A*, 446, 1027
- Dahn, C. C., Harris, H. C., Vrba, F. J., et al. 2002, *AJ*, 124, 1170
- Delfosse, X., Forveille, T., Perrier, C., & Mayor, M. 1998, *A&A*, 331, 581
- Enoch, M. L., Brown, M. E., & Burgasser, A. J. 2003, *AJ*, 126, 1006
- Fan, X., Knapp, G. R., Strauss, M. A., et al. 2000, *AJ*, 119, 928
- Geballe, T. R., Knapp, G. R., Leggett, S. K., et al. 2002, *ApJ*, 564, 466
- Gelino, C. R., Marley, M. S., Holtzman, J. A., Ackerman, A. S., & Lodders, K. 2002, *ApJ*, 577, 433
- Gizis, J. E., Monet, D. G., Reid, I. N., Kirkpatrick, J. D., Liebert, J., & Williams, R. J. 2000, *AJ*, 120, 1085
- Goldman, B. 2003, *IAU Symposium 211, Brown Dwarfs*, ed. Eduardo L. Martín, (San Francisco: ASP), 461
- Gray, D. F. 1992, *The observation and analysis of stellar photospheres*, second edition (Cambridge Univ. Press)
- Joergens, V., & Guenther, E. 2001, *A&A*, 379, L9
- Jones, H. R. A., Pavlenko, Ya., Viti, S., Barber, R. J., Yakovina, L. A., Pinfield, D., & Tennyson, J. 2005, *MNRAS*, 358, 105
- Kirkpatrick, J. D., Henry, T. J., & Simons, D. A. 1995, *ApJ*, 109, 797
- Kirkpatrick, J. D., Henry, T. J., & Irwin, M. J. 1997, *AJ*, 113, 1421
- Kirkpatrick, J. D., Reid, I. N., Liebert, J., et al. 1999, *ApJ*, 519, 802
- Kirkpatrick, J. D., Reid, I. N., Liebert, J., et al. 2000, *AJ*, 120, 447
- Koen, C. 2005, *MNRAS*, 360, 1132
- Leggett, S. K. 1992, *ApJS*, 82, 351
- Leggett, S. K., Allard, F., Dahn, C., Hauschildt, P. H., Kerr, T. H., & Rayner, J. 2000a, *ApJ*, 535, 965
- Leggett, S. K., Geballe, T. R., Fan, X., et al. 2000b, *ApJ*, 536, L35
- Liebert, J., Kirkpatrick, J. D., Cruz, K. L., Reid, I. N., Burgasser, A., Tinney, C. G., & Gizis, J. E. 2003, *AJ*, 125, 343
- Luhman, K. L., Briceño, C., Rieke, G. H., & Hartmann, L. 1998, *ApJ*, 493, 909
- Marcy, G. W., & Chen, G. H. 1992, *ApJ*, 390, 550
- Martín, E. L., Basri, G., Gallegos, J. E., Rebolo, R., Zapatero Osorio, M. R., & Béjar, V. J. S. 1998, *ApJ*, 499, L61
- Martín, E. L., Delfosse, X., Basri, G., Goldman, B., Forveille, T., & Zapatero Osorio, M. R. 1999, *AJ*, 118, 2466
- Martín, E. L., Zapatero Osorio, M. R., & Lehto, H. 2001, *ApJ*, 557, 822
- Mohanty, S., & Basri, G. 2003, *ApJ*, 583, 451
- Mohanty, S., Jayawardhana, R., & Basri, G. 2005, *ApJ*, 626, 498

- Mokler, F., & Stelzer, B. 2002, *A&A*, 391, 1025
- Muzerolle, J., Hillenbrand, L., Calvet, N., Briceño, C., & Hartmann, L. 2003, *ApJ*, 592, 266
- Nakajima, T., Tsuji, T., & Yanagisawa, K. 2004, *ApJ*, 607, 499
- Phan-Bao, N., Bessell, M. S., Martín, E. L., et al. 2006, *MNRAS*, 366, L40
- Pokorny, R. S., Jones, H. R. A., & Hambly, N. C. 2003, *A&A*, 397, 575
- Preibisch, T., McCaughrean, M. J., Grosso, N., et al. 2005, *ApJS*, 160, 582
- Preibisch, T., & Zinnecker, H. 2002, *AJ*, 123, 1613
- Reid, I. N., Kirkpatrick, J. D., Gizis, J. E., Dahn, C. C., Monet, D. G., Williams, R. J., Liebert, J., & Burgasser, A. J. 2000, *AJ*, 119, 369
- Reid, I. N., Kirkpatrick, J. D., Liebert, J., Gizis, J. E., Dahn, C. C., & Monet, D. G. 2002, *AJ*, 124, 519
- Reiners, A., & Basri, G. 2006, *AJ*, 131, 1806
- Ribas, I. 2003, *A&A*, 400, 297
- Scholz, A., & Eislöffel, J. 2004, *A&A*, 419, 249
- Scholz, A., & Eislöffel, J. 2005, *A&A*, 429, 1007
- Scholz, A., Jayawardhana, R., Eislöffel, J., & Froebrich, D. 2005, *AN*, 326, 895
- Schweitzer, A., Gizis, J. E., Hauschildt, P. H., Al-lard, F., Reid, I. N. 2001, *ApJ*, 555, 368
- Smith, V. V., Tsuji, T., Hinkle, K. H., Cunha, K., Blum, R. D., Valenti, J. A., Ridgway, S. T., Joyce, R. R., & Bernath, P. 2003, *ApJ*, 599, L107
- Stauffer, J. R., Balachandran, S. C., Krishnamurthi, A., Pinsonneault, M., Terndrup, D. M., & Stern, R. A. 1997, *ApJ*, 475, 604
- Stauffer, J. R., Schultz, G., & Kirkpatrick, J. D. 1998, *ApJ*, 499, L199
- Strauss, M. A., Fan, X., Gunn, J. E., et al. 1999, *ApJ*, 522, L61
- Tinney, C. G. 1998, *MNRAS*, 296, L42
- Tinney, C. G., & Reid, I. N. 1998, *MNRAS*, 301, 1031
- Tsvetanov, Z. I., Golimowski, D. A., Zheng, W., et al. 2000, *ApJ*, 531, L61
- Van Biesbroeck, G. 1961, *AJ*, 51, 66
- Vrba, F. J., Henden, A. A., Luginbuhl, C. B., et al. 2004, *AJ*, 127, 2948
- Zapatero Osorio, M. R., Caballero, J. A., Béjar, V. J. S., & Rebolo, R. 2003, *A&A*, 408, 663
- Zapatero Osorio, M. R., Lane, B. R., Pavlenko, Ya, Martín, E. L., Britton, M., & Kulkarni, S. R. 2004, *ApJ*, 615, 958

This 2-column preprint was prepared with the AAS L^AT_EX macros v5.2.

TABLE 1
KECK/NIRSPEC OBSERVING LOG.

Object	Obs. date	Slit name	Echelle (deg)	Exp. time (s)	Airmass	Reference
PP11	2005 Oct 26	0.432×12	63.00	3×480	1.01	1
	2005 Oct 28	0.432×12	63.00	3×420	1.02	
vB10	2001 Jun 15	0.576×12	63.00	2×300	1.14	2
	2001 Nov 02	0.432×12	63.29	8×120	1.40	
DENIS-P J033411.39−495333.6 ^a	2005 Oct 26	0.432×12	63.00	6×300	2.86	3
	2005 Oct 28	0.432×12	63.00	3×300	2.86	
LP 944−20	2000 Dec 12	0.432×12	63.00	3×200	1.89	4
	2005 Oct 26	0.432×12	63.00	6×300	1.86	
	2005 Oct 27	0.432×12	63.00	6×300	1.75	
	2005 Oct 28	0.432×12	63.00	6×300	1.76	
	2005 Oct 29 ^b	0.432×12	63.00	1×300	1.80	
2MASS J00361617+1821104	2004 Dec 05	0.432×12	63.00	6×300	1.06	5
	2005 Oct 28	0.432×12	63.00	3×300	1.11	
2MASS J22244381−0158521	2001 Jun 15	0.576×12	63.00	2×600	1.09	6
SDSS J053951.99−005902.0	2001 Nov 02	0.432×12	62.78	8×300	1.30	7
	2005 Oct 27	0.432×12	63.00	3×480	1.15	
2MASS J17281150+3948593AB	2001 Jun 15	0.576×12	63.00	2×900	1.33	6
2MASS J16322911+1904407	2001 Jun 15	0.576×12	63.00	2×900	1.37	8
DENIS-P J0255.0−4700	2005 Oct 27	0.432×12	63.00	3×420	2.53	9
SDSSp J125453.90−012247.4	2006 Jan 19	0.432×12	63.00	9×600	1.09	10
2MASS J05591914−1404488	2001 Nov 02	0.432×12	62.78	8×300	1.39	11
	2004 Dec 05	0.432×12	63.00	2×300	1.36	
	2005 Oct 26	0.432×12	63.00	3×480	1.18	
	2005 Oct 27	0.432×12	63.00	3×480	1.27	
	2005 Oct 28	0.432×12	63.00	3×480	1.24	
2MASS J15031961+2525196	2006 Jan 19	0.432×12	63.00	2×300	1.07	12
SDSS J162414.37+002915.6	2001 Jun 15	0.576×12	63.00	2×900	1.13	13
SDSS J134646.45−003150.4	2001 Jun 15	0.576×12	63.00	3×900	1.14	14
2MASS J15530228+1532369	2001 Jun 15	0.576×12	63.00	2×900	1.04	15
2MASS J12171110−0311131	2001 Jun 15	0.576×12	63.00	2×900	1.15	16
GL 570D	2001 Jun 15	0.576×12	63.00	2×900	1.45	17
2MASS J04151954−0935066	2005 Oct 26	0.432×12	63.00	2×600	1.18	15

^aIt is also LEHPM 3396 (Pokorny, Jones, & Hamby (2003)).

^bCloudy, low transparency. Not used for $v_{\text{rot}} \sin i$ determination.

References. — (1) Stauffer et al. (1998); (2) Van Biesbroeck (1961); (3) Pokorny et al. (2003); (4) Tinney (1998); (5) Reid et al. (2000); (6) Kirkpatrick et al. (2000); (7) Fan et al. (2000); (8) Kirkpatrick et al. (1999); (9) Martín et al. (1999); (10) Leggett et al. (2000b); (11) Burgasser et al. (2000a); (12) Burgasser et al. (2003); (13) Strauss et al. (1999); (14) Tsvetanov et al. (2000); (15) Burgasser et al. (2002b); (16) Burgasser et al. (1999); (17) Burgasser et al. (2000b).

TABLE 2
SPECTROSCOPIC ROTATION VELOCITIES OF OUR SAMPLE.

Object	SpT	Template object		Previous (km s ⁻¹)	Reference
		vB 10 (km s ⁻¹)	J1346-00 (km s ⁻¹)		
PP11	M6.5	20.7±2.4	...	18.5±1.5	1
vB 10	M8V	6.5	2
DENIS-P J033411.39-495333.6	M9	≤15	...		
LP 944-20	M9V	30.3±1.5	...	30.0±2.5, 28, 28.3, 31	2,3,4,5,6
2MASS J00361617+1821104	L3.5V/L4V	36.0±2.7	...	38, 15	6,7
2MASS J22244381-0158521	L4.5V	30.3±3.4	31.1±2.2	20.9-29.2	8
SDSS J053951.99-005902.0	L5V	32.3±3.6	34.0±3.4		
2MASS J17281150+3948593AB	L7V	25.1±7.2	23.3±2.8		
2MASS J16322911+1904407	L8V/L7.5V/dL6	22.6±6.7	20.9±7.0	30±10	2,3
DENIS-P J0255.0-4700	L9V/ /dL6	40.8±8.0	41.1±2.8	40±10	2,3
SDSSp J125453.90-012247.4	T2V	29.5±5.0	27.3±2.5		
2MASS J05591914-1404488	T4.5V	25.4±5.0	20.1±4.8		
2MASS J15031961+2525196	T5V	31.4±5.0	32.8±2.0		
SDSS J162414.37+002915.6	T6V	34.6±5.0	38.5±2.0		
SDSS J134646.45-003150.4	T6.5V	≤15	...		
2MASS J15530228+1532369AB	T7V	...	29.4±2.3		
2MASS J12171110-0311131	T7V/T8V	...	31.4±2.1		
GL 570D	T7.5V/T8V	32.8±5.0	28.6±2.4		
2MASS J04151954-0935066	T8V	...	33.5±2.0		

NOTE.—Spectroscopic rotation velocities are $v_{\text{rot}} \sin i$ measurements.

References. — (1) Martín et al. (1998); (2) Mohanty & Basri (2003); (3) Basri et al. (2000); (4) Reid et al. (2002); (5) Tinney & Reid (1998); (6) Jones et al. (2005); (7) Schweitzer et al. (2001); (8) Bailer-Jones (2004).

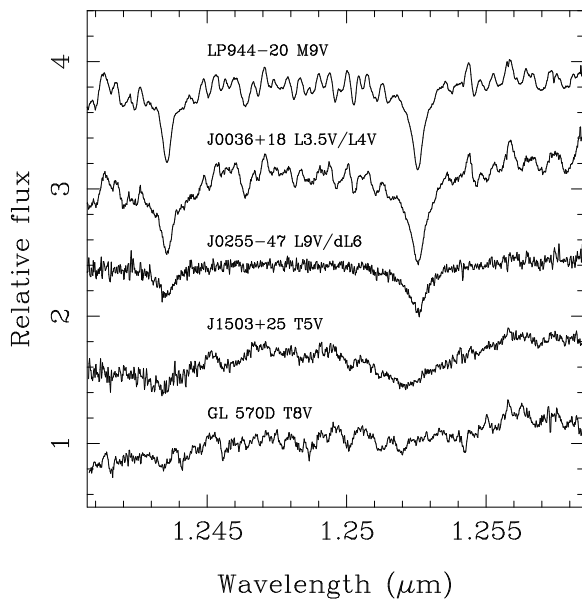


Fig. 1.— NIRSPEC spectra of some of our targets. The most prominent features of the M and L dwarfs are due to K I absorption, which vanishes at late-T types. Spectra are normalized to unity in the interval 1.2475–1.2490 μm and offset by 0.7 on the vertical axis. All spectra are shifted in velocity to vacuum wavelengths.

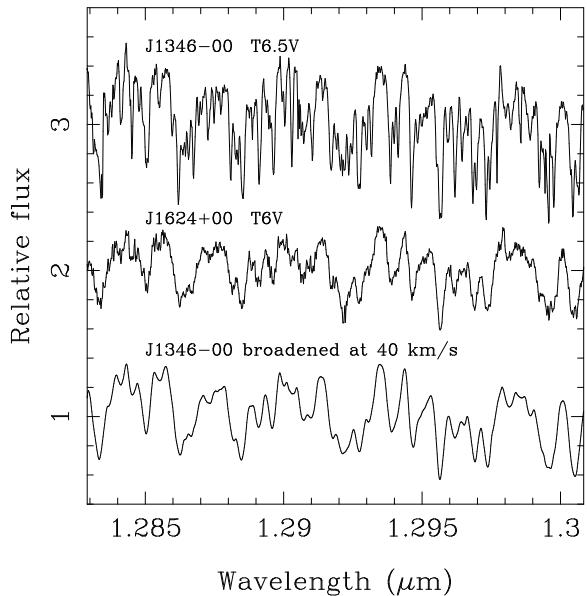


Fig. 2.— NIRSPEC spectra of the brown dwarf J1346–00 (T6.5V, low $v_{\text{rot}} \sin i$, top) and the rapid rotator J1624+00 (T6V, middle). The spectrum of J1624+00 has been shifted in velocity to match J1346–00 for a facile comparison of features. The spectrum of J1346–00 convolved with a rotation profile of 40 km s^{-1} is shown at the bottom. Data are scaled to a common vertical range and offset by unity on the vertical axis for clarity.

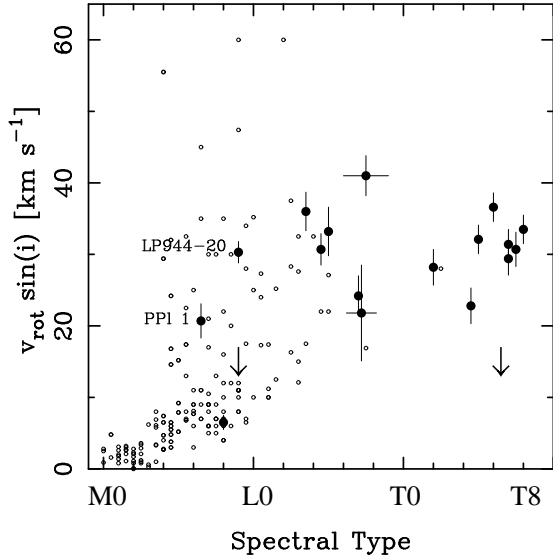


Fig. 3.— Spectroscopic rotation velocities of M-, L- and T-type dwarfs. Our sample is plotted as filled circles and arrows denoting positive detections and upper limits, respectively. The two known young dwarfs of our sample are labeled. The datum of ν B 10 (M8V), one of the template sources for rotation velocity measurement, is taken from Mohanty & Basri (2003). Two L dwarfs show large error bars in spectral type to account for their different classifications found in the literature. Small open circles correspond to data (positive detections) from the literature (see text). We note that a large fraction of M0–M4 stars have non-detections ($v_{\text{rot}} \sin i \leq 5 \text{ km s}^{-1}$), and their upper limits are not plotted here for clarity.

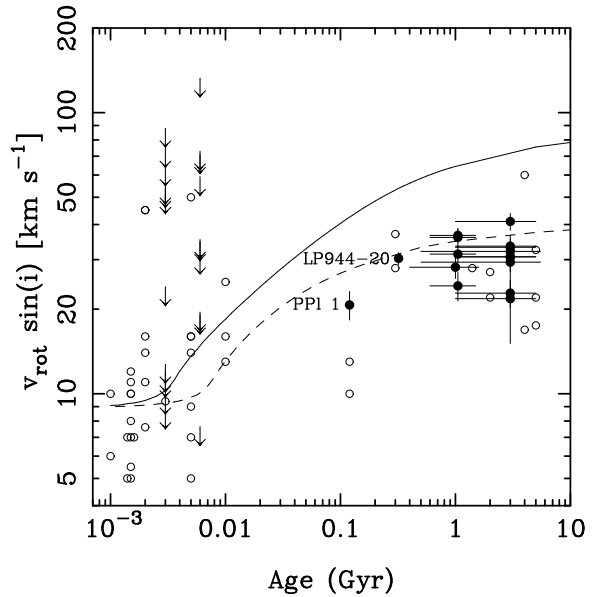


Fig. 4.— Projected rotation velocity as a function of age for brown dwarfs with likely masses in the interval $30\text{--}70 M_{\text{Jup}}$. Our data (PPI 1, LP 944–20, and field dwarfs later than L3.5V) are plotted as filled circles. Data from the literature (see text for details) are shown with open circles and arrows (upper limits). The curves trace the hydrostatic contraction of brown dwarfs with $60 M_{\text{Jup}}$ (solid line) and $30 M_{\text{Jup}}$ (dashed line), which have a rotation velocity of 9 km s^{-1} at the age of 1 Myr.